

To Ask or Not To Ask: Human-in-the-loop Contextual Bandits with Applications in Robot-Assisted Feeding

Rohan Banerjee¹, Rajat Kumar Jenamani^{*1}, Sidharth Vasudev^{*1},
Amal Nanavati², Katherine Dimitropoulou³, Sarah Dean^{†1}, Tapomayukh Bhattacharjee^{†1}

Abstract— Robot-assisted bite acquisition involves picking up food items with varying shapes, compliance, sizes, and textures. Fully autonomous strategies may not generalize efficiently across this diversity. We propose leveraging feedback from the care recipient when encountering novel food items. However, frequent queries impose a workload on the user. We formulate human-in-the-loop bite acquisition within a contextual bandit framework and introduce LINUCB-QG, a method that selectively asks for help using a predictive model of querying workload based on query types and timings. This model is trained on data collected in an online study involving 14 participants with mobility limitations, 3 occupational therapists simulating physical limitations, and 89 participants without limitations. We demonstrate that our method better balances task performance and querying workload compared to autonomous and always-querying baselines and adjusts its querying behavior to account for higher workload in users with mobility limitations. We validate this through experiments in a simulated food dataset and a user study with 19 participants, including one with severe mobility limitations. Please check out our project website at: emprise.cs.cornell.edu/hilbiteacquisition/.

I. INTRODUCTION

Feeding, an essential Activity of Daily Living (ADL) [1], is challenging for individuals with mobility limitations, often requiring caregiver support that may not be readily available. Approximately 1 million people in the U.S. cannot eat without assistance [2], so robotic systems could empower these individuals to feed themselves, promoting independence. Robot-assisted feeding comprises two key tasks [3]: bite acquisition [4]–[7], the task of picking up food items, and bite transfer [8, 9], delivering them to the user’s mouth. Our work focuses on bite acquisition, aiming to learn policies that robustly acquire novel food items with diverse properties.

With over 40,000 unique food items in a typical grocery store [10], bite acquisition strategies must generalize well to novel food items. Current approaches formulate bite acquisition as a contextual bandit problem [5, 6], using online learning techniques like LINUCB [11] to adapt to unseen food items. However, these methods may need many samples to learn the optimal action, which is problematic due to food fragility and potential user dissatisfaction from failures [12].

Our key insight is that we can leverage the care recipient’s presence to develop querying strategies that can adapt to



Fig. 1: We present a human-in-the-loop contextual bandit-based framework for robot-assisted bite acquisition and propose a novel method which decides whether to ask for help or autonomously act, by considering both certainty about action performance, and the estimated workload imposed on the human by querying.

novel foods, giving users a sense of agency. Under the assumption that the human can specify the robot’s acquisition action, we extend the contextual bandit formulation to include human-in-the-loop querying [13]. However, excessive querying may overwhelm users and reduce acceptance [14]. Thus, our key research question is: How do we balance imposing *minimal querying workload* on the user while achieving *maximal bite acquisition success* in a human-in-the-loop contextual bandit framework?

Balancing querying workload requires accurately estimating the workload imposed on users. Existing methods rely on physiological sensors [15]–[17], which can be invasive. We develop a non-intrusive, data-driven method by conducting a study on 14 participants with mobility limitations, 3 occupational therapists (OTs) who simulate the physical limitations of those with mobility limitations, and 89 participants without mobility limitations. We gather data on how different query types and timings impact self-reported workload using a modified NASA-TLX scale [18]. We tailor queries to common autonomous system failures, ranging from multiple-choice questions to open-ended prompts for acquisition strategy suggestions.

Using this data, we train a model to predict user workload in response to queries, considering the nature of the query and the user’s prior query interactions with the system. We observe statistically significant differences in self-reported workload between users with and without mobility limitations, which are accounted for by our learned models.

*Equal Contribution, †Equal Advising.

¹Department of Computer Science, Cornell University {rbb242, rj277, sv355, sdean, tapomayukh}@cornell.edu

²Department of Computer Science and Engineering, University of Washington, Seattle, WA 98195 {amaln}@cs.washington.edu

³Columbia University, New York City, NY, USA, kd2524@cumc.columbia.edu

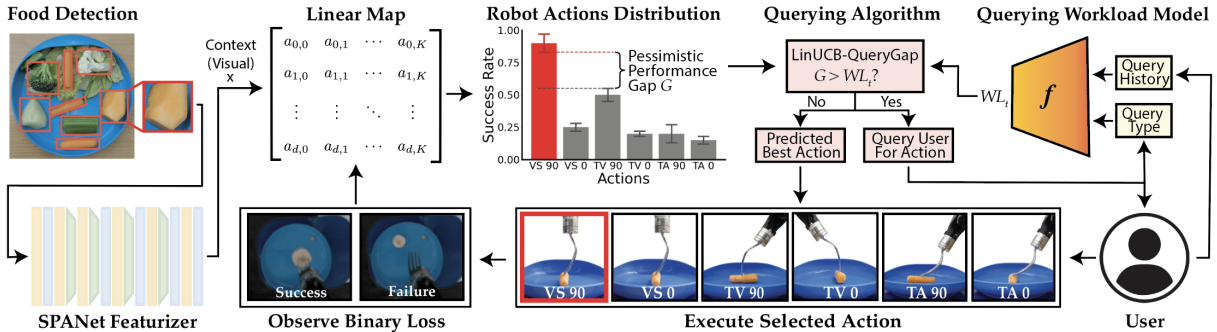


Fig. 2: Human-in-the-loop contextual bandit pipeline for deciding whether to query (a_q) or autonomously select a robot action a_r . Our proposed method, LINUCB-QG, takes into account action uncertainty as measured by the performance gap G between the best and the second best robot action and incorporates a learned querying workload model (f) to predict the workload of querying the human WL_t .

Building on our workload model, we propose LINUCB-QUERYGAP (LINUCB-QG), a novel algorithm for human-in-the-loop contextual bandits. It decides when to query based on the estimated querying workload and performance uncertainty of candidate actions. Simulated experiments on a dataset of 16 food items [4] show that LINUCB-QG better balances querying workload and bite acquisition success compared to three baselines: (i) LINUCB [5], a state-of-the-art fully autonomous approach; (ii) ALWAYSQUERY, which always queries; and (iii) LINUCB-EXPDECAY, a naive querying algorithm. LINUCB-QG achieves higher task performance than LINUCB and LINUCB-EXPDECAY, with lower querying workload than ALWAYSQUERY and LINUCB-EXPDECAY. It also queries less when using a workload model trained on users with mobility limitations, indicating sensitivity to the workload differences across diverse user populations.

We validate our method in a real-world user study with 19 individuals, including one with Multiple Sclerosis, using three foods with variable material properties: banana slices, baby carrots, and cantaloupe. LINUCB-QG achieves a statistically significant 26% higher task success compared to LINUCB, and a 47% lower change in querying workload compared to ALWAYSQUERY.

Our contributions are as follows:

- A human-in-the-loop contextual bandit framework incorporating querying workload for bite acquisition.
- A dataset (including users with mobility limitations) on how feeding-related queries affect workload, and a predictive workload model without exteroceptive sensor inputs.
- A novel method, LINUCB-QG, that balances acquisition success and querying frequency using our workload model, shown through simulations and a real-world study with 19 users, including one with severe mobility limitations.

II. RELATED WORK

Human-in-the-loop algorithms. Our problem is an instance of learning to defer to an expert [19], where an agent decides whether to act autonomously or defer to experts like humans or oracle models. Most approaches operate in supervised learning [19]–[22] or reinforcement learning domains [23]. Given the constraints of robot-assisted bite acquisition (observing independent contexts and receiving sparse feedback) we focus on learning-to-defer policies in an

online contextual bandit setting. While prior methods often assume a fixed cost for querying the expert [20]–[22] or deal with imperfect experts [21], we propose estimating a time-varying deferral penalty using a data-driven model.

Other research explores active learning in robotics [24]–[26], where agents decide which instances to query [25, 26] or which type of feedback to solicit [24]. Some algorithms balance task performance and human querying cost, but our work differs by using a data-driven model of querying cost and applying it to the complex task of bite acquisition.

Querying workload modeling. Our algorithms need to monitor and predict workload to avoid over-querying users. For individuals with mobility limitations, querying workload may involve physical [27] and cognitive components [18], depending on the query type. Most workload estimation literature relies on neurological or physiological signals (such as ECG/heart rate, respiration [27], physical posture [28] for physical workload, and EEG [15], EDA [29], pupil metrics [17, 30] for cognitive workload) and trains supervised models based on these signals. However, measuring such signals requires specialized, often invasive equipment. Alternatively, workload can be estimated post-hoc using subjective metrics like the NASA-TLX survey [15].

In contrast, we develop a data-driven predictive model of querying workload using self-reported, modified NASA-TLX survey results, without relying on specialized sensors. Our model estimates the expected workload of a query based on interaction history, timing, and query type. Additionally, unlike prior work [15, 17, 29, 30], we focus on workload estimation for users with mobility limitations.

III. PROBLEM FORMULATION

Following previous work [5, 6], we formulate bite acquisition as a contextual bandit problem. At each timestep, the learner receives a context x_t (food item), and selects actions $a_t \in \mathcal{A}$ that minimize regret over T timesteps:

$$\sum_{t=1}^T \mathbb{E}[r_t | x_t, a_t^*, t] - \sum_{t=1}^T \mathbb{E}[r_t | x_t, a_t, t]$$

where r_t is the reward, $a_t^* \triangleq a^*(x_t)$ is the optimal action maximizing r_t for x_t , and expectations are over the stochasticity in r_t . In our problem setting, we assume access to a dataset D from a robotic manipulator, consisting of observations $o \in \mathcal{O}$, actions $a \in \mathcal{A}$, and binary rewards r .

This dataset is used to pretrain and validate our algorithms, but is not required for our online setting. Our contextual bandit setting is characterized by (see Appendix for more details):

- **Observation space** \mathcal{O} : RGB images of single bite-sized food items on a plate, sampled from 16 food types [4].
- **Action space** \mathcal{A} : 7 actions in total: 6 robot actions a_r shown in Fig. 2 (bottom) [4, 31], and 1 query action a_q .
- **Context space** \mathcal{X} : Lower-dimensional context x derived from observations o using SPANet [4], with dimensionality $d = 2048$. As our bandit algorithms assume a linear relationship between x and the expected reward $\mathbb{E}[r]$, we use the penultimate activations of SPANet as our context since the final layer of SPANet is linear [5].

When the learner selects a robot action a_r , it receives a binary reward indicating success for context x_t . If the learner selects a_q , it receives the optimal robot action $a^*(x_t)$ from the human. It then executes that action and receives the corresponding reward. Querying imposes a workload penalty on the learner, given by the human’s latent querying workload state WL_t at time t .

We model the total expected reward $\mathbb{E}[r_t|x_t, a_t, t]$ as the sum of the expected task reward $r_{task}(x_t, a_t)$ (the probability that action a_t succeeds for food context x_t) and the expected querying workload reward $r_{WL}(x_t, a_t, t)$ associated with selecting query actions a_q :

$$\mathbb{E}[r_t|x_t, a_t, t] \triangleq w_{task}r_{task}(x_t, a_t) + (1 - w_{task})r_{WL}(x_t, a_t, t)$$

where w_{task} is a scalar weight in $[0, 1]$. We define $r_{task}(x_t, a_t)$ to be $s_x(x_t, a_t)$ if $a_t = a_r$, and $s_x(x_t, a^*(x_t))$ if $a_t = a_q$, where $s_x(x_t, a_t)$ is the probability that action a succeeds for context x . We define $r_{WL}(x_t, a_t, t)$ to be 0 if $a_t = a_r$, and $-WL_t$ if $a_t = a_q$. Our goal is to learn a policy $\pi(a|x, t)$ that maximizes $\sum_{t=1}^T \mathbb{E}[r_t|x_t, a_t, t]$.

IV. QUERYING WORKLOAD MODELING

Our human-in-the-loop contextual bandit algorithms rely on estimating the querying workload state WL_t (Sec. III). To estimate WL_t , we first conduct a user study to understand how querying workload responds to requests for help (Sec. IV-A). We then learn a predictive model of querying workload using this data (Sec. IV-C).

A. Querying Workload User Study

We design a user study (shown in Fig. 3) to capture how different types of queries affect an individual’s querying workload in robotic caregiving scenarios. In such scenarios, a feeding system may request various forms of assistance from the user or caregiver, such as semantic labels, bounding boxes for food items, or explanations for failed acquisition attempts. These response types can have varying impacts on querying workload [13, 32].

For instance, a semantic label response may impose less workload than an open-ended response. In addition, the end-user of the system and the caregiver may be busy with other tasks, such as watching TV while eating. We conduct an online user study that captures the above factors to determine

how an individual’s querying workload changes in response to requests for assistance from an autonomous system.

Participants perform a distraction task while periodically receiving queries from a “robot,” simulating realistic caregiving situations where users might be engaged in other activities. The robot queries represent realistic assistance requests during bite acquisition. We vary four independent variables hypothesized to impact querying workload:

- 1) Robot query difficulty (d_t): 2 options – easy or hard.
- 2) Distraction task difficulty ($dist_t$): 3 options – no distraction task, an easy numeric addition task, or a hard video transcription task.
- 3) Time interval between queries (ΔT): 2 options – either 1 minute or 2 minutes.
- 4) Response type ($resp_t$): 3 options – (a) a multiple-choice question (MCQ) asking for a semantic label, (b) asking the user to draw a bounding box (BB) around a food item, or (c) an open-ended (OE) question asking the user to explain why an acquisition attempt failed.

Each participant experiences 12 study conditions, one for each of the 2 settings of d_t , 3 settings of $dist_t$, and 2 settings of ΔT , with the entire study taking roughly 1.5 hr. During each condition, lasting 5.5 minutes, participants engage in distraction tasks and respond to robot queries (with varying response types $resp_t$) as shown in Fig. 3. We measure self-reported workload (our dependent variable) after each robot query and at the end of each condition using 5 modified NASA-TLX subscales [18, 33] (mental/physical, temporal, performance, effort, frustration), each measured on a 5-point Likert scale (see Appendix for exact question wording).

We collect data from 14 users (7 male, 7 female; ages 27-50) with mobility limitations resulting from a diverse range of medical conditions: spinal muscular atrophy (SMA), quadriplegia, arthrogryposis, cerebral palsy, Ullrich congenital muscular dystrophy, schizencephaly with spastic quadriplegia, spinal cord injury (including C2 and C3 quadriplegia). We additionally collect data from 3 occupational therapists (OTs), (3 female; ages 23-26), trained to simulate right/left hemiplegia (stroke). The OTs positioned one side of their body in full shoulder adduction, and elbow flexion to allow only 30 degrees of functional elbow joint range. Finally, we collect data from 89 users without mobility limitations (40 male, 49 female; ages 19-68). The population size for users with limitations is larger than the median ($n = 6$) in studies of assistive robots [34, 35].

B. Data Analysis

We consider three distinct datasets under which to train the workload model: D_1 , which only includes the data from the 89 users without mobility limitations; D_2 , which only includes the data from the 14 users with mobility limitations and 3 OTs; and $D_{1,2}$, which includes both D_1 and D_2 . We convert the modified NASA-TLX responses into a single querying workload score by normalizing responses to 3 of the questions, and taking a weighted average (weight details in Appendix). We find a statistically significant difference in mean querying workload between D_1 (0.36 ± 0.29) and D_2

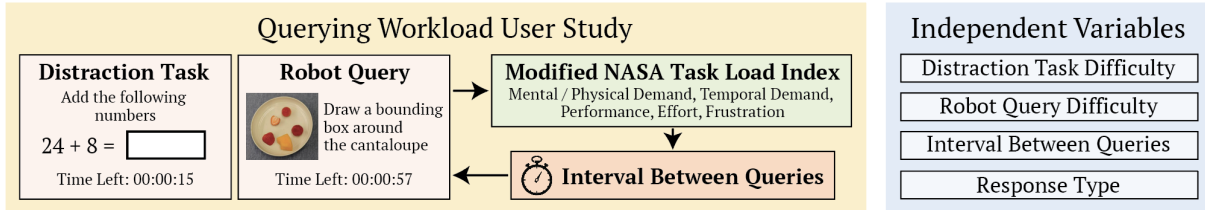


Fig. 3: *Left*: Querying workload user study setup, illustrating the format of the distraction task and robot query task, and the modified NASA-TLX survey recorded after every robot query. *Right*: Independent variables that affect user’s querying workload varied in the study. (0.40 ± 0.28), as described in the Appendix.

C. Querying Workload Predictive Model

We develop a predictive model of querying workload based on the user study data (Sec. IV-A). Our models operate in discrete time, where the time variable t refers to an integer number of timesteps since the beginning of a condition, where each timestep corresponds to a fixed time spacing Δt (set to 10s in our experiments). The model has the form $WL_t = f(WL_0, Q_t; \theta)$, where WL_0 is the initial workload, $Q_t = \{(d_{t'}, resp_{t'}, dist_{t'})\}_{t'=1}^t$ is the history of previous queries (where d_t , $resp_t$, and $dist_t$ are the query variables defined in Sec. IV-A), and θ are the model parameters.

Linear discrete-time models. To capture the dependency between the current workload and the query history Q_t , we choose to use a linear predictive workload model inspired by Granger causality models [36, 37]:

$$WL_t = \gamma WL_0 + \sum_{i=0}^{H-1} \mathbf{w}_i^T [d_{t-i}, resp_{t-i}, dist_{t-i}] + w_0$$

where \mathbf{w}_i represents the effect of the query asked i timesteps in the past on the workload at the current time t , H is the history length, and w_0 is a bias term. We train the model using linear regression, where we convert d_t , $resp_t$, and $dist_t$ into features using one-hot encodings, and generate a training pair for each robot task query in our study (see Appendix for more details about the Granger models).

Model selection. We train models f_1 , f_2 , and $f_{1,2}$, corresponding to the datasets D_1 , D_2 , and $D_{1,2}$, respectively (Sec. IV-B).¹ The models $f_{i,sim}$ and $f_{i,real}$ indicate models learned for the simulation experiments and the real-world user study, respectively. For our simulation experiments, we learn 3 separate models $f_{1,sim}$, $f_{2,sim}$, and $f_{1,2,sim}$ (details in the Appendix). For our real-world user study, we only use 2 of the 3 real models: $f_{1,real}$ for the users without limitations and $f_{1,2,real}$ for the users with limitations. In our setting, $f_{1,real}$ and $f_{1,2,real}$ are models chosen based on cross-validation median test MSE on D_1 and $D_{1,2}$, respectively. Please see the Appendix for full model selection details, including cross-validation performance values. We also train a model $f_{2,real}$ (cross-validation score: 0.066 ± 0.022), which has a higher mean and standard deviation MSE than $f_{1,2,real}$ (cross-validation score: 0.058 ± 0.010). This suggests that training only on D_2 leads to a higher-variance, less accurate model, compared to training on $D_{1,2}$. Thus,

¹When training these models, our assumptions about the time taken for users to complete the modified TLX surveys, particularly for users without mobility limitations, are in the Appendix.

it is still helpful to consider the data from users without limitations (D_1) when training our workload models.

V. HUMAN-IN-THE-LOOP ALGORITHMS

We develop decision-making algorithms that decide whether to ask for help or act autonomously, using the learned workload models in Sec. IV-C. Specifically, we consider four human-in-the-loop contextual bandit algorithms: one fully autonomous and three that can query the human.

Fully autonomous algorithm. Our fully autonomous baseline is LinUCB [11], the state-of-the-art for acquiring unseen bite-sized food items like banana and apple slices [5, 6]. LinUCB selects the action that maximizes a reward upper-confidence bound (UCB) estimate for each robot action, given by $UCB_{a_r} = \theta_{a_r}^T x + \alpha b_{a_r}$. Here, θ_{a_r} is the linear parameter vector learned through regression on contexts X_{a_r} and observed rewards for actions a_r , where X_{a_r} includes contexts seen for a_r during pretraining and online validation. The term $\alpha > 0$ corresponds to a confidence level, and $b_{a_r} = (x^T (X_{a_r}^T X_{a_r} + \lambda I)^{-1} x)^{1/2}$ is the UCB bonus with L_2 regularization strength λ . The size of αb_{a_r} reflects the reward estimate uncertainty for the given context-action pair.

Algorithm 1 LINUCB-QG.

- 1: Inputs: Context x , scaling factor w , time t , initial workload WL_0 , workload model f , model parameters θ
- 2: For all a_r : compute UCB bonus and value: (b_{a_r}, UCB_{a_r}) .
- 3: Let $a^* = \arg \max_{a_r} \theta_{a_r}^T x$, $a^- = \arg \max_{a_r \neq a^*} \theta_{a_r}^T x$
- 4: Define $G \triangleq (\theta_{a^-}^T x + \alpha b_{a^-}) - (\theta_{a^*}^T x - \alpha b_{a^*})$
- 5: Set $a = \begin{cases} a_q & \text{if } G > wf(WL_0, Q_t; \theta) \\ \arg \max_{a_r} UCB_{a_r} & \text{otherwise} \end{cases}$
- 6: **return** a

Querying algorithms. The three querying algorithms decide to query the human or select the robot action that maximizes UCB_{a_r} .

- 1) ALWAYSQUERY, which always queries the user.
- 2) LINUCB-EXPDECAY, which queries with an exponentially-decaying probability (decay rate c) that depends on the number of food items seen within an episode (details in Appendix).
- 3) LINUCB-QUERY-GAP (LINUCB-QG), defined in Algorithm 1, which queries if the worst-case performance gap between the best action a^* and second-best action a^- exceeds the predicted workload, with scaling factor w .

In LINUCB-QG, the worst-case gap is the difference between a pessimistic estimate of a^* ’s reward and an optimistic estimate of a^- ’s reward, considering their confidence intervals (illustrated in Fig. 2, top). A larger gap indicates a

	$r_{task,avg}$	M_{wt}	f_q
Workload Model $f_{1,sim}$			
-LINUCB	0.35 ± 0.15	0.44 ± 0.06	-
-ALWAYSQUERY	0.64 ± 0.19	0.46 ± 0.05	1 ± 0
-LINUCB-EXPDECAY	0.39 ± 0.17	0.46 ± 0.07	0.44 ± 0.15
-LINUCB-QG	0.48 ± 0.18	0.48 ± 0.04	0.80 ± 0.22
Workload Model $f_{2,sim}$			
-LINUCB	0.35 ± 0.15	0.44 ± 0.06	-
-ALWAYSQUERY	0.64 ± 0.19	0.16 ± 0.22	1 ± 0
-LINUCB-EXPDECAY	0.31 ± 0.12	0.42 ± 0.06	0.16 ± 0.15
-LINUCB-QG	0.35 ± 0.15	0.44 ± 0.06	0.08 ± 0.10
Workload Model $f_{1,2,sim}$			
-LINUCB	0.35 ± 0.15	0.42 ± 0.06	-
-ALWAYSQUERY	0.64 ± 0.19	0.16 ± 0.22	1 ± 0
-LINUCB-EXPDECAY	0.31 ± 0.12	0.38 ± 0.11	0.16 ± 0.15
-LINUCB-QG	0.40 ± 0.12	0.43 ± 0.05	0.44 ± 0.27

TABLE I: Querying algorithms simulated on the test set, corresponding to $w_{task} = 0.4$, for 3 different data regimes in the workload model, averaged across 5 seeds. Values for $r_{task,avg}$ and ΔWL correspond to the hyperparameter setting with maximal M_{wt} on the validation set (for each separate data setting).

higher risk that the predicted best arm may be suboptimal, increasing the odds that the benefit of querying outweighs the workload penalty WL_t . Therefore, querying only when the gap is sufficiently large helps balance the tradeoff between task reward and querying workload.

We define the predicted workload penalty to be the counterfactual querying workload WL_t if we were to query at the current time. To estimate this, we condition our workload model on the specific query type that we consider in our simulations and real-robot user study. Thus, we use $WL_t = f(WL_0, Q_t; \theta)$, where we set the query type variables to be $d_t = \text{easy}$, $resp_t = \text{MCQ}$, $dist_t = \text{“no distraction task”}$ for all t where the selected action $a_t = a_q$.

VI. EXPERIMENTS

We evaluate the performance of our human-in-the-loop algorithms using two setups: (i) a simulation testbed (Section VI-A), and (ii) a real world user study, including 18 human subjects without mobility limitations, and one human subject with mobility limitations (Section VI-B). We evaluate our algorithms on the following surrogate objective, adapted from the expected reward $\mathbb{E}[r_t|x_t, a_t, t]$ (Sec. III):

$$w_{task} \left[\frac{1}{T} \sum_{t=1}^T r_{task}(x_t, a_t) \right] - (1 - w_{task})(WL_t - WL_0)$$

where WL_0 and WL_t are the initial and final workload (see Appendix for more details).

A. Simulated Testbed

We simulate food interaction using a dataset of bite-sized food items on plates, including 16 food types [4], each with 30 trials for the 6 robot actions a_r . We first draw a random image of a given food type from the dataset and generate the corresponding context x using SPANet. When the policy selects a robot action a_r , we sample a binary task reward r from a Bernoulli distribution with success probability $s_x(x, a_r)$. If $r = 1$, we declare that the bandit has converged, and move to a new food type at the next timestep. If $r = 0$, we draw a new random image of the same food type from the dataset until we exceed the maximum number of

attempts $N_{att} = 10$. When the policy selects a query action a_q , the bandit policy repeatedly executes the optimal action $a^*(x)$ until convergence, or the limit N_{att} is reached.

Metrics. For each algorithm, we compute a set of 5 objective metrics to evaluate the tradeoff between task performance and querying workload. We compute the mean episodic task reward $r_{task,avg} = \frac{1}{T} \sum_{t=1}^T r_{task}(x_t, a_t)$, which measures the efficiency of successful food acquisition. We also compute the episodic change in querying workload $\Delta WL = WL_T - WL_0$. We compute our surrogate objective $M_{wt} = w_{task}r_{task,avg} - (1 - w_{task})\Delta WL$, where w_{task} represents a user-specific preference for the task performance/querying workload tradeoff. We additionally report the number of timesteps taken to converge t_{conv} , which provides additional insights into task performance, and the fraction of food items for which we queried f_q , which provides an insight into querying workload.

Evaluating querying workload in simulation. In our simulation environment, we use the learned workload model f for both LINUCB-QG action-selection, as well as computing the evaluation metrics ΔWL and M_{wt} . During the rollout of a particular bandit policy, we evolve the workload model state WL_t according to the learned model when we query. We consider the three dataset scenarios and corresponding workload models $f_{1,sim}$, $f_{2,sim}$, and $f_{1,2,sim}$ (Sec. IV-C), and set $WL_0 = 0.5$ (a median initial workload).

Pretrain, validation, and test sets. In our experiments, we partition the set of 16 food types into a pretraining set (for the contextual bandit and for training SPANet), a validation set (for tuning the querying algorithm hyperparameters), and a test set (for metric evaluation). Our validation set (cantaloupe, grape) and test set (banana, carrot) include food items with varying material properties. Our pretraining set includes the remaining 12 food types in the food dataset. We use the validation set to select the hyperparameter that maximizes the weighted metric M_{wt} given a w_{task} setting.

Results. We investigate how LINUCB-QG balances the tradeoff between task reward and querying workload. Table I compares the four algorithms for a setting corresponding to a slight preference for minimizing workload over maximizing task performance ($w_{task} = 0.4$). Across all three workload data settings, LINUCB-QG has a higher mean task reward $r_{task,avg}$ than LINUCB and LINUCB-EXPDECAY, and a higher mean weighted metric M_{wt} than all methods, suggesting that it achieves the best tradeoff between task reward and querying workload. Additionally, the querying fraction f_q for LINUCB-QG is smallest in the D_2 setting, followed by the $D_{1,2}$ setting, followed by the D_1 setting, suggesting that LINUCB-QG is sensitive to the higher workload predictions with care recipient and OT data, while still trading off task reward and querying workload.

Experiment: generalization on D_2 . We run an additional experiment to ablate D_2 , where at test time we use either $f_{1,sim}$ or $f_{1,2,sim}$ in LINUCB-QG action-selection, but use $f_{2,sim}$ for metric evaluation. We find that M_{wt} is lower in the first setting (0.27 ± 0.16) compared to the second setting (0.46 ± 0.05), suggesting that including D_2 is crucial to

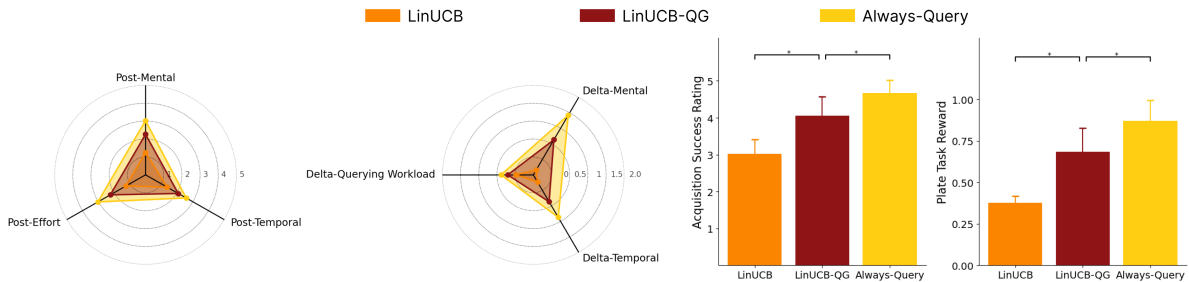


Fig. 4: Real-world user study results. *Left*: LINUCB-QG significantly reduces querying workload compared to ALWAYS-QUERY as shown by three post-method metrics and three changes in workload metrics. *Right*: LINUCB-QG significantly outperforms LINUCB in bite acquisition success, as demonstrated by both subjective and objective success metrics. Error bars indicate standard error.

achieve the best trade-off for users with mobility limitations. See Appendix for more details and comparison metrics.

B. Real-World User Study

To evaluate the effectiveness of LINUCB-QG in trading off task performance with querying workload in the real world, we conduct a user study including 19 users: 18 users (8 male, 10 female; ages 19-31) without mobility limitations, and one 46-year old user who has had Multiple Sclerosis since they were 19. Of the users without limitations, 66% had previous experience interacting with robots. We investigate whether LINUCB-QG achieves improved task performance compared to LINUCB, while still minimizing querying workload compared to ALWAYS-QUERY. This study was approved by the Institutional Review Board at Cornell University (Protocol #IRB0010477).

Study setup. We use a Kinova Gen-3 6-DoF robot arm with a Robotiq 2F-85 gripper, equipped with a custom feeding tool (details in Appendix). For each method, we present the user with a plate of 3 food items (banana, carrot, and cantaloupe). We give each method a maximum of 3 acquisition attempts to ensure a reasonable study duration. When the human is queried, they provide feedback using a speech-to-text interface. Users evaluate each of the three methods in sequence in a counterbalanced order. We measure the querying workload before and after each method by asking a series of 5 questions that are modified NASA-TLX subscales: mental/physical, temporal, performance, effort and frustration (exact question wording in Appendix). We conduct 2 repetitions of the 3 food items for all 3 methods, for a total of 18 food trials. We select cantaloupe, carrot and banana because they embody diverse characteristics salient for acquisition, such as shape and compliance, and offer unique challenges: cantaloupe can be acquired with any of the six robot actions; carrots, being hard and thin, necessitate actions that can apply sufficient penetration force and have fork tines perpendicular to the food’s major axis; bananas are soft, requiring the tilted-angled actions [5].

Metrics. We define 7 subjective and 3 objective metrics to compare the methods. 4 subjective metrics directly correspond to the modified NASA-TLX questions after each method, and are denoted Post-Mental, Post-Temporal, Post-Performance, and Post-Effort. The other 3 subjective metrics measure changes in the workload during each method: Delta-Mental, Delta-Temporal, and Delta-Querying Workload (the change in querying workload score, using the weighting

function described in the Appendix). The 3 objective metrics are mean episodic task reward per plate ($r_{task,avg}$), mean number of successes per plate ($n_{success}$), and mean number of query timesteps per plate (n_q).

Overall results. Among the three methods, LINUCB-QG offers the most balanced approach to human-in-the-loop bite acquisition. It is more efficient than LINUCB and imposes less querying workload than ALWAYS-QUERY. While LINUCB typically picks up the carrot or cantaloupe within 1-2 timesteps but struggles with the banana, ALWAYS-QUERY successfully picks up food in the first timestep by always querying the user, leading to higher workload. Our method, LINUCB-QG, selectively asks for help with the banana and acts autonomously for the other foods in most trials, balancing task performance with querying workload.

1) *Task success results:* Fig. 4 (right) shows that LINUCB-QG achieves higher objective and subjective success ratings versus LINUCB, showing greater efficiency.

2) *Querying workload results:* As illustrated in Fig. 4 (left), LINUCB-QG has lower subjective querying workload scores (mental, temporal, and effort subscales) compared to ALWAYS-QUERY, indicating that selective querying reduces workload. All results are statistically significant (Wilcoxon paired signed-rank test, $\alpha = 0.05$). Full comparisons across all metrics are provided in the Appendix.

Results: user with mobility limitations. We highlight observations from the user with mobility limitations. First, they provided a higher mean subjective success rating for LINUCB-QG than for LINUCB, aligning with the aggregate results. However, the user provided consistently low physical/mental, temporal and effort ratings across all methods. Potential reasons for this include the relative simplicity of providing feedback in our setting, and the fact that this particular user frequently requests assistance in daily life, reducing their querying workload. The user also commented that relying on external physiological signals (such as EEG) to estimate workload would add stress (due to the additional hardware required), reinforcing the benefit of non-intrusive workload models for human-in-the-loop querying algorithms.

Discussion. Future work could explore incorporating different types of queries in the real-robot study, beyond just the best acquisition action. Additionally, another promising direction would be to explore predictive models that include objective, non-intrusive measurements of querying workload.

REFERENCES

- [1] S. Katz, A. B. Ford, R. W. Moskowitz, B. A. Jackson, and M. W. Jaffe, "Studies of illness in the aged: The index of adl: A standardized measure of biological and psychosocial function," *jama*, vol. 185, no. 12, pp. 914–919, 1963.
- [2] M. W. Brault, "Americans with disabilities: 2010," *Current population reports*, vol. 7, pp. 70–131, 2012.
- [3] R. Madan, R. K. Jenamani, V. T. Nguyen, *et al.*, "Sparcs: Structuring physically assistive robotics for caregiving with stakeholders-in-the-loop," in *2022 IEEE/RSJ International Conference on Intelligent Robots and Systems (IROS)*, IEEE, 2022, pp. 641–648.
- [4] R. Feng, Y. Kim, G. Lee, *et al.*, "Robot-assisted feeding: Generalizing skewering strategies across food items on a plate," in *The International Symposium of Robotics Research*, Springer, 2019, pp. 427–442.
- [5] E. K. Gordon, X. Meng, T. Bhattacharjee, M. Barnes, and S. S. Srinivasa, "Adaptive robot-assisted feeding: An online learning framework for acquiring previously unseen food items," in *2020 IEEE/RSJ International Conference on Intelligent Robots and Systems (IROS)*, IEEE, 2020, pp. 9659–9666.
- [6] E. K. Gordon, S. Roychowdhury, T. Bhattacharjee, K. Jamieson, and S. S. Srinivasa, "Leveraging post hoc context for faster learning in bandit settings with applications in robot-assisted feeding," in *2021 IEEE International Conference on Robotics and Automation (ICRA)*, IEEE, 2021, pp. 10 528–10 535.
- [7] P. Sundaresan, S. Belkhale, and D. Sadigh, "Learning visuo-haptic skewering strategies for robot-assisted feeding," in *6th Annual Conference on Robot Learning*, 2022.
- [8] D. Gallenberger, T. Bhattacharjee, Y. Kim, and S. S. Srinivasa, "Transfer depends on acquisition: Analyzing manipulation strategies for robotic feeding," in *2019 14th ACM/IEEE International Conference on Human-Robot Interaction (HRI)*, IEEE, 2019, pp. 267–276.
- [9] S. Belkhale, E. K. Gordon, Y. Chen, S. Srinivasa, T. Bhattacharjee, and D. Sadigh, "Balancing efficiency and comfort in robot-assisted bite transfer," in *2022 International Conference on Robotics and Automation (ICRA)*, IEEE, 2022, pp. 4757–4763.
- [10] A. Malito, "Grocery stores carry 40,000 more items than they did in the 1990s," *MarketWatch*, June, vol. 17, 2017.
- [11] L. Li, W. Chu, J. Langford, and R. E. Schapire, "A contextual-bandit approach to personalized news article recommendation," in *Proceedings of the 19th international conference on World wide web*, 2010, pp. 661–670.
- [12] T. Bhattacharjee, E. K. Gordon, R. Scalise, *et al.*, "Is more autonomy always better? exploring preferences of users with mobility impairments in robot-assisted feeding," in *Proceedings of the 2020 ACM/IEEE international conference on human-robot interaction*, 2020, pp. 181–190.
- [13] Y. Cui, P. Koppol, H. Admoni, *et al.*, "Understanding the relationship between interactions and outcomes in human-in-the-loop machine learning," in *International Joint Conference on Artificial Intelligence*, 2021.
- [14] T. Fong, C. Thorpe, and C. Baur, "Robot, asker of questions," *Robotics and Autonomous systems*, vol. 42, no. 3–4, pp. 235–243, 2003.
- [15] S. Shayesteh and H. Jebelli, "Investigating the impact of construction robots autonomy level on workers' cognitive load," in *Canadian Society of Civil Engineering Annual Conference*, Springer, 2021, pp. 255–267.
- [16] A. Aygun, T. Nguyen, Z. Haga, S. Aeron, and M. Scheutz, "Investigating methods for cognitive workload estimation for assistive robots," *Sensors*, 2022.
- [17] L. Fridman, B. Reimer, B. Mehler, and W. T. Freeman, "Cognitive load estimation in the wild," in *Proceedings of the 2018 chi conference on human factors in computing systems*, 2018, pp. 1–9.
- [18] S. G. Hart and L. E. Staveland, "Development of nasa-tlx (task load index): Results of empirical and theoretical research," in *Advances in psychology*, vol. 52, Elsevier, 1988, pp. 139–183.
- [19] M. Raghu, K. Blumer, G. Corrado, J. Kleinberg, Z. Obermeyer, and S. Mullainathan, "The algorithmic automation problem: Prediction, triage, and human effort," *arXiv preprint arXiv:1903.12220*, 2019.
- [20] V. Keswani, M. Lease, and K. Kenthapadi, "Towards unbiased and accurate deferral to multiple experts," in *Proceedings of the 2021 AAAI/ACM Conference on AI, Ethics, and Society*, 2021, pp. 154–165.
- [21] H. Narasimhan, W. Jitkrittum, A. K. Menon, A. Rawat, and S. Kumar, "Post-hoc estimators for learning to defer to an expert," *Advances in Neural Information Processing Systems*, vol. 35, pp. 29 292–29 304, 2022.
- [22] H. Mozannar and D. Sontag, "Consistent estimators for learning to defer to an expert," in *International Conference on Machine Learning*, PMLR, 2020, pp. 7076–7087.
- [23] S. Joshi, S. Parbhoo, and F. Doshi-Velez, "Learning-to-defer for sequential medical decision-making under uncertainty," *arXiv preprint arXiv:2109.06312*, 2021.
- [24] T. Fitzgerald, P. Koppol, P. Callaghan, *et al.*, "Inquire: Interactive querying for user-aware informative reasoning," in *6th Annual Conference on Robot Learning*, 2022.
- [25] M. Racca, A. Oulasvirta, and V. Kyrki, "Teacher-aware active robot learning," in *2019 14th ACM/IEEE International Conference on Human-Robot Interaction (HRI)*, IEEE, 2019, pp. 335–343.
- [26] A. Li and T. Silver, "Embodied active learning of relational state abstractions for bilevel planning," *arXiv preprint arXiv:2303.04912*, 2023.
- [27] J. B. Smith, P. Baskaran, and J. A. Adams, "Decomposed physical workload estimation for human-robot teams," in *2022 IEEE 3rd International Conference on Human-Machine Systems (ICHMS)*, IEEE, 2022, pp. 1–6.
- [28] C. E. Harriott, T. Zhang, and J. A. Adams, "Assessing physical workload for human-robot peer-based teams," *International Journal of Human-Computer Studies*, vol. 71, no. 7–8, pp. 821–837, 2013.
- [29] A. Rajavenkatanarayanan, H. R. Nambiappan, M. Kyrarini, and F. Makedon, "Towards a real-time cognitive load assessment system for industrial human-robot cooperation," in *2020 29th IEEE International Conference on Robot and Human Interactive Communication (RO-MAN)*, IEEE, 2020, pp. 698–705.
- [30] M. I. Ahmad, J. Bernotat, K. Lohan, and F. Eyssele, "Trust and cognitive load during human-robot interaction," *arXiv preprint arXiv:1909.05160*, 2019.
- [31] T. Bhattacharjee, G. Lee, H. Song, and S. S. Srinivasa, "Towards robotic feeding: Role of haptics in fork-based food manipulation," *IEEE Robotics and Automation Letters*, vol. 4, no. 2, pp. 1485–1492, 2019.
- [32] P. Koppol, H. Admoni, and R. G. Simmons, "Interaction considerations in learning from humans," in *IJCAI*, 2021, pp. 283–291.
- [33] M. Hertzum, "Reference values and subscale patterns for the task load index (tlx): A meta-analytic review," *Ergonomics*, vol. 64, no. 7, pp. 869–878, 2021.
- [34] J. Mankoff, G. R. Hayes, and D. Kasnitz, "Disability studies as a source of critical inquiry for the field of assistive technology," in *Proceedings of the 12th international ACM SIGACCESS conference on Computers and accessibility*, 2010, pp. 3–10.
- [35] A. Nanavati, V. Ranganeni, and M. Cakmak, "Physically assistive robots: A systematic review of mobile and manipulator robots that physically assist people with disabilities," *Annual Review of Control, Robotics, and Autonomous Systems*, vol. 7, 2023.
- [36] C. W. Granger, "Investigating causal relations by econometric models and cross-spectral methods," *Econometrica: journal of the Econometric Society*, pp. 424–438, 1969.
- [37] T. Liang and B. Recht, "Randomization inference when n equals one," *arXiv preprint arXiv:2310.16989*, 2023.
- [38] M. Selvaggio, M. Cagnetti, S. Nikolaidis, S. Ivaldi, and B. Siciliano, "Autonomy in physical human-robot interaction: A brief survey," *IEEE Robotics and Automation Letters*, vol. 6, no. 4, pp. 7989–7996, 2021.
- [39] S. Nikolaidis, Y. X. Zhu, D. Hsu, and S. Srinivasa, "Human-robot mutual adaptation in shared autonomy," in *Proceedings of the 2017 ACM/IEEE International Conference on Human-Robot Interaction*, 2017, pp. 294–302.
- [40] S. Jain and B. Argall, "Probabilistic human intent recognition for shared autonomy in assistive robotics," *ACM Transactions on Human-Robot Interaction (THRI)*, vol. 9, no. 1, pp. 1–23, 2019.
- [41] A. Pichler, S. C. Akkaladevi, M. Ikeda, *et al.*, "Towards shared autonomy for robotic tasks in manufacturing," *Procedia Manufacturing*, vol. 11, pp. 72–82, 2017.
- [42] R. K. Jenamani, P. Sundaresan, M. Sakr, T. Bhattacharjee, and D. Sadigh, *Flair: Feeding via long-horizon acquisition of realistic dishes*, Under submission to Robotics: Science and Systems (RSS) 2024.

- [43] S. Liu, Z. Zeng, T. Ren, *et al.*, “Grounding dino: Marrying dino with grounded pre-training for open-set object detection.” *arXiv preprint arXiv:2303.05499*, 2023.
- [44] A. Kirillov, E. Mintun, N. Ravi, *et al.*, “Segment anything,” in *Proceedings of the IEEE/CVF International Conference on Computer Vision*, 2023, pp. 4015–4026.

C. Additional Related Work

1) *Additional Related Work on Shared Autonomy*: A number of papers explore another domain within human-in-the-loop learning referred to as shared autonomy [38]. In this problem setting, the policies of a robotic agent and human user are combined to influence decision-making for a particular task. Shared autonomy approaches differ in the types of information that they infer about the human, such as the goals of the human [39, 40], and also in the degree to which human input guides the autonomous system [41]. Our work differs in that our approach selects an action from either the agent or the human without blending the two, and we incorporate a human querying workload model distinct from human intent.

D. Problem Formulation

1) *Details on Contextual Bandit Setting*: Below we provide more details on the contextual bandit setting.

- **Observation space** \mathcal{O} : In each RGB image, the food item is either isolated, close to the plate edge, or on top of another food item [4].
- **Action space** \mathcal{A} : Each robot action a_r is a pair consisting of one of three pitch configurations (tilted angled (TA), vertical skewer (VS), tilted vertical (TV)) and one of two roll configurations (0° , 90°), relative to the orientation of the food [4, 31].
- **Context space** \mathcal{X} : SPANet, the network from which we derive our contexts x , is pretrained in a fully-supervised manner to predict $s_o(o, a)$, the probability that action a succeeds for observation o .

E. Querying Workload User Study

1) *NASA-TLX weighting function*: Throughout the paper, we define the querying workload state WL to be the following weighted sum of the raw NASA-TLX subscales: $WL = 0.4 \cdot \text{mental} + 0.2 \cdot \text{temporal} + 0.4 \cdot \text{effort}$.

2) *Modified NASA-TLX Subscale Questions*: Below are the question wordings that we use in our online workload user study, which are modified versions of the NASA-TLX subscales:

- **Mental/Physical Demand**: “How mentally or physically demanding was the task?”
- **Temporal Demand**: “How hurried or rushed was the pace of the task?”
- **Performance**: “How successful were you in accomplishing what you were asked to do?”
- **Effort**: “How hard did you have to work to accomplish your level of performance?”
- **Frustration**: “How irritated, stressed, and annoyed were you?”

Note that for the users without mobility limitations, the wording of the Mental/Physical Demand task was the following: “How mentally demanding was the task?”. This is because we assumed that the physical demand to answer the workload questions was minimal for users without mobility limitations.

3) *Baseline conditions*: 2 baseline conditions. Each baseline condition corresponds to a fixed setting of $dist_t$ (either easy addition, or hard video transcription), without any robot query tasks.

4) *Sample study questions*: Below we provide examples of the robot queries that we ask in the online querying workload user study, covering each of the possible response types r_t and question difficulties d_t :

- $r_t = \text{MCQ}$, $d_t = \text{easy}$: “What kind of food item is outlined in the image below?” (Responses: “Raspberry”, “Strawberry”, “Grape”, “Apple”, “I don’t know.”)
- $r_t = \text{BB}$, $d_t = \text{easy}$: “Draw a box around only the strawberry.”
- $r_t = \text{OE}$, $d_t = \text{easy}$: “Why did the Robot fail in acquiring the cantaloupe?”
- $r_t = \text{MCQ}$, $d_t = \text{hard}$: “Which of the following images is tofu?” (Responses: “Left”, “Right”, “I don’t know”)
- $r_t = \text{BB}$, $d_t = \text{hard}$: “Draw a box around only the carrot in the bottom right.”
- $r_t = \text{OE}$, $d_t = \text{hard}$: “How would you skewer the following item with a fork?”

5) *Compensation*: Users without mobility limitations were compensated at a rate of \$12/hr, for a total compensation of \$18 for the entire study (as the study duration was 1.5 hr). The occupational therapists who simulated mobility limitations were compensated at a rate of \$10/hr, for a total compensation of \$15 for the entire study. The users with mobility limitations were compensated at a rate of \$20/hr, for a total compensation of \$30 for the entire study.

6) *Mean querying workload difference, D_1 vs D_2* : In Section IV-B, we describe finding a statistically significant difference in mean querying workload between D_1 (users without limitations) and D_2 (users with limitations and OTs), where D_1 had a mean querying workload of 0.36 ± 0.29 , and D_2 had a mean querying workload of 0.40 ± 0.28 . We run a Mann-Whitney U-test on the querying workload scores from D_1 and D_2 . The alternative hypothesis that we tested is that the distribution of workload values for D_1 is stochastically less than the distribution of workload values for D_2 . For this alternative hypothesis, we find that $p = 5.410e-05$, indicating a statistically significant result for $\alpha = 0.05$.

F. Querying Workload Predictive Model

1) *Modified TLX survey timing information*: When training the workload models, we make the following assumption about the amount of time taken for users to complete the modified TLX surveys. In the D_1 setting, we assume 0 seconds for the full user population (which only includes users without mobility limitations). In the $D_{1,2}$ setting, we assume 5 seconds for users without mobility limitations (and for two users in the D_2 population for whom we did not collect time data), and for the rest of the users with mobility limitations, we used the logged time taken to complete the surveys. Our justification for this design choice is that in the $D_{1,2}$ setting, we would like the assumed time for users without mobility limitations to be appropriately scaled compared to the logged times for users with limitations, who

took non-zero times to complete the surveys.

2) *Discrete-time Models*: We consider different values of H , with one memoryless Granger model (where $H = 1$) and a set of Granger models with H ranging from 5 to 30. We chose the upper bound of $H = 30$ to roughly correspond to the study condition length in Section IV-A. This is because we set each discrete time step to correspond to 10s. We zero-pad the query variables $[d_{t-i}, resp_{t-i}, dist_{t-i}]$ if there are no queries in the discrete time window $t - i$, or if we run out of history.

For each of these models, we also consider variants where we impose non-negativity constraints and/or ridge-regression penalties on the weights γ and \mathbf{w}_i^T . Specifically, we consider 4 different variants:

- Granger: no nonnegativity or ridge-regression penalty
- Granger-Nonnegative (Granger-N): nonnegativity constraint only
- Granger-Ridge (Granger-R): ridge-regression penalty only
- Granger-Ridge-Nonnegative (Granger-RN): non-negativity constraint and ridge-regression penalty

3) *Continuous-time Models*: We also consider a continuous-time setting, where $WL(t)$ represents the querying workload at time t . In this setting, we consider one model (denoted as Exp-Impulse) that models the workload at the current time t as composed of a series of impulses at the query times, with an exponential decay in workload in between the queries. The Exp-Impulse model is defined recursively as follows:

$$WL(t) = WL(t_{prev})e^{-\lambda(t-t_{prev})} + \beta(d_t, r_t, dist_t)$$

where t_{prev} is the previous timestep at which we queried, $\beta(d_t, r_t, dist_t)$ is the magnitude of the impulse, and λ is the workload decay rate.

4) *Model Selection*: For each of the three dataset settings ($D_1, D_2, D_{1,2}$), we perform 4-fold cross-validation to select a model from the above set of linear models. Dataset D_1 consists of $N = 4272$ unique question/workload pairs, while dataset D_2 consists of $N = 705$ unique question/workload pairs. For tuning of the ridge regression regularization parameter λ_r , we perform 5-fold cross validation to select the optimal parameter value, with a logarithmic range from 10^{-3} to 10^2 .

Table II shows predictive MSE statistics on the held-out test splits, computed across the 4 folds, for the set of learned models. Note that we also considered a constant baseline (denoted Constant), whose predicted workload is $WL_t = WL_0$, and an average baseline (denoted Average), whose predicted workload is the average value of WL_0 in the training set.

Real-world user study models. We describe the two simulated workload models ($f_{1,real}, f_{1,2,real}$) that are used for the real-world experiments in Section VI-B, along with the mobility limitation-only model $f_{2,real}$ that is described in Section IV-C. The model $f_{1,real}$ is a Granger model with $H = 5$, with a ridge-regression penalty on γ and

\mathbf{w}_i^T , where the final selected ridge regression penalty was $\lambda_r = 10$. The model $f_{2,real}$ is a Granger model with $H = 1$. The model $f_{1,2,real}$ is a Granger model with $H = 1$ and a ridge-regression penalty on γ and \mathbf{w}_i^T , where the final selected ridge regression penalty was $\lambda_r = 10$. The model $f_{1,real}$ achieves a cross-validation mean test MSE of 0.0573 ± 0.0127 on D_1 , while $f_{1,2,real}$ achieves a cross-validation mean test MSE of 0.0582 ± 0.0099 on the $D_{1,2}$ dataset.

We use these models because they are the models with the lowest median test MSE on each dataset. We initially considered using mean test MSE to select the best-performing model, but we discovered that the mean test MSE had a very large magnitude for certain models. This is because for the model settings that do not have weight constraints, linear regression would overfit to the training set and learn model parameters with large weight magnitudes. Because of this, we use the median test MSE to select the model. Note that while the models have differences in their mean test MSE, the standard deviations in test MSE for the models overlap because of the variance across folds.

Simulated models. We describe the three simulated workload models ($f_{1,real}, f_{2,real}, f_{1,2,real}$) that are used in the experiments in Section VI-A. For all three models, we use Granger models with $H = 10$, where we place the following constraints on the parameters during model training: $\gamma, \{\mathbf{w}_i^T\}_{i=0}^{H-1} \in [0.05, 1], w_0 \leq 1$. Placing these additional constraints guarantees that the predicted change in workload associated with a query is non-negative.

G. Human-in-the-Loop Algorithms

We provide the full algorithmic description for LINUCB-EXPDECAY in Algorithm 2.

Algorithm 2 LINUCB-EXPDECAY.

- 1: Inputs: Context x , decay rate c , number of food items seen N , time t
 - 2: For all robot actions a_r , compute UCB bonus b_{a_r} and UCB value UCB_{a_r} .
 - 3: Set $P(query) = e^{-cN}$ if t is the first timestep to observe x , $P(query) = 0$ otherwise.
 - 4: Set $a = a_q$ with probability $P(query)$, $a = \arg \max_{a_r} UCB_{a_r}$ with probability $1 - P(query)$.
 - 5: **return** a
-

H. Experiments: Simulated Testbed

1) *Surrogate Objective*: Here we justify our choice of the surrogate objective outlined in Section VI. Recall that the expected reward $\mathbb{E}[r_t|x_t, a_t, t]$ defined in Section III depends explicitly on the querying workload WL_t for all times t for which $a_t = a_q$. However, measuring the intermediate workload values after every query would require administering a survey after each query, which is impractical in the real world. Therefore, in our experimental formulation in both simulation and in the real study, we will assume that we cannot observe the intermediate workload values. Instead,

Model	H	D_1		D_2		$D_{1,2}$	
		Test MSE ($\mu \pm \sigma$)	Test MSE (median)	Test MSE ($\mu \pm \sigma$)	Test MSE (median)	Test MSE ($\mu \pm \sigma$)	Test MSE (median)
Constant Average	0	0.1271 \pm 0.0173	0.1304	0.104 \pm 0.0245	0.112	0.123 \pm 0.0164	0.124
	0	0.0937 \pm 0.0086	0.0922	0.089 \pm 0.0319	0.0933	0.0919 \pm 0.00806	0.0944
Granger	1	0.0572 \pm 0.0126	0.0507	0.066 \pm 0.0219	0.0761	0.0583 \pm 0.00988	0.0573
	5	7.59e+15 \pm 1.31e+16	0.0656	3.95e+23 \pm 6.68e+23	1.38e+22	3.66e+16 \pm 6.34e+16	0.0581
	10	3.16e+18 \pm 5.47e+18	0.0661	1.08e+24 \pm 1.88e+24	2.24e+20	3.38e+15 \pm 5.86e+15	0.058
	15	1.87e+17 \pm 3.23e+17	0.0660	2.08e+21 \pm 3.23e+21	3.23e+20	3.45e+15 \pm 5.98e+15	0.0582
	20	5.41e+17 \pm 9.37e+17	0.0663	2.43e+24 \pm 4.21e+24	1.72e+21	1.92e+12 \pm 3.32e+12	0.0584
	25	1.39e+18 \pm 2.41e+18	0.0668	5.05e+23 \pm 7.95e+23	7.11e+22	3.07e+21 \pm 5.32e+21	0.0587
	30	1.09e+20 \pm 1.89e+20	0.0677	1e+24 \pm 1.34e+24	3.64e+23	5.78e+21 \pm 1e+22	0.059
Granger-N	1	0.0573 \pm 0.0126	0.0507	0.0662 \pm 0.0217	0.0762	0.0584 \pm 0.00997	0.0576
	5	0.0575 \pm 0.0128	0.0508	0.0665 \pm 0.0215	0.0763	0.0586 \pm 0.0101	0.0576
	10	0.0575 \pm 0.0128	0.0508	0.0682 \pm 0.0199	0.0769	0.0585 \pm 0.00997	0.0576
	15	0.0574 \pm 0.0126	0.0508	0.0698 \pm 0.0196	0.0784	0.0586 \pm 0.00985	0.0578
	20	0.0575 \pm 0.0127	0.0508	0.0705 \pm 0.0204	0.0798	0.0588 \pm 0.00982	0.0581
	25	0.0577 \pm 0.0126	0.0508	0.0726 \pm 0.0211	0.0819	0.0589 \pm 0.00991	0.0582
	30	0.0578 \pm 0.0125	0.0510	0.0735 \pm 0.0205	0.083	0.0591 \pm 0.00994	0.0583
Granger-R	1	0.0572 \pm 0.0127	0.0507	0.066 \pm 0.0219	0.0763	0.0582 \pm 0.00988	0.0572
	5	0.0573 \pm 0.0127	0.0506	0.0663 \pm 0.0216	0.0772	0.0584 \pm 0.0099	0.0576
	10	0.0574 \pm 0.0125	0.0509	0.0675 \pm 0.0217	0.0783	0.0584 \pm 0.00964	0.0574
	15	0.0574 \pm 0.0124	0.0512	0.0691 \pm 0.0219	0.0801	0.0584 \pm 0.00948	0.0575
	20	0.0575 \pm 0.0124	0.0512	0.0687 \pm 0.0221	0.0795	0.0588 \pm 0.00939	0.0582
	25	0.0579 \pm 0.0123	0.0514	0.0694 \pm 0.0223	0.0801	0.0589 \pm 0.00951	0.0583
	30	0.0582 \pm 0.0122	0.0515	0.0694 \pm 0.0222	0.0801	0.0591 \pm 0.00956	0.0583
Granger-RN	1	0.0573 \pm 0.0126	0.0508	0.0719 \pm 0.0246	0.0819	0.0589 \pm 0.0105	0.0574
	5	5.66e+24 \pm 9.80e+24	0.0655	9.96e+21 \pm 1.73e+22	1.6e+15	5.88e+24 \pm 1.02e+25	4.02e+15
	10	0.6120 \pm 0.9559	0.0658	5.16e+14 \pm 8.94e+14	0.0894	0.0607 \pm 0.0112	0.061
	15	0.0573 \pm 0.0125	0.0508	5.62e+12 \pm 9.73e+12	0.0862	0.0589 \pm 0.0104	0.0574
	20	0.0574 \pm 0.0125	0.0509	3.46e+13 \pm 3.49e+13	3.15e+13	4.45e+04 \pm 7.71e+04	0.0676
	25	0.1189 \pm 0.1179	0.0514	1.1e+14 \pm 1.9e+14	0.0895	0.059 \pm 0.0104	0.0575
	30	0.1195 \pm 0.1021	0.0662	1.92e+14 \pm 2.7e+14	5.65e+13	0.059 \pm 0.0104	0.0575
Exp-Impulse	-	0.0737 \pm 0.0128	0.0678	0.0809 \pm 0.0199	0.0878	0.0753 \pm 0.0112	0.0766

TABLE II: Test mean-squared error (MSE) values for querying workload models, for all three workload data settings (D_1 , D_2 , $D_{1,2}$). For each data setting, the model with the lowest median test MSE is indicated in bold.

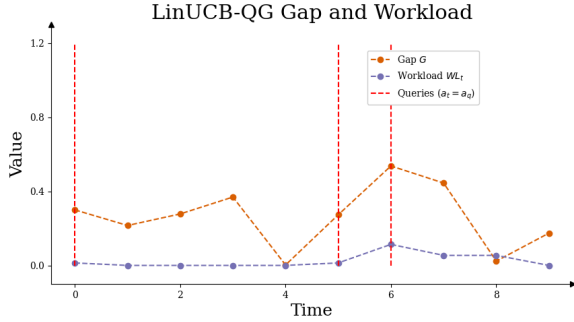


Fig. 5: Example LinUCB-QG rollout in simulation environment, illustrating evolution of performance gap G and workload WL_t , along with timesteps corresponding to query times. LinUCB-QG decides to ask the human for help when $G > wWL_t$ (in this rollout, $w = 4$).

we will observe only the initial and final workload values, which are WL_0 and $WL_T = f(WL_0, Q_T; \theta)$, respectively.

2) *Additional Results:* First, we include a set of additional metrics for the experimental setting described in Section VI-A, which focus on the observed convergence for each food item. We define the following metrics: $f_{fail, food}$, which is the fraction of food items for which the algorithm was unable to converge; and $f_{auto, food}$, which is the fraction of food items for which the algorithm autonomously converged. We also show ΔWL , the change in querying workload across an episode and t_{conv} , the number of timesteps required to

converge to the optimal action. Table III shows these metrics for $w_{task} = 0.4$.

Next, we include full results for multiple settings of w_{task} and w_{cl} , for the same querying workload models used in Section VI-A, ranging from $w_{task} \in \{0.2, 0.3, \dots, 0.9\}$ shown in Tables IV, V, and VI (excluding $w_{task} = 0.4$, whose results are shown in Table I). We see that LINUCB-QG generally performs the best for lower values of w_{task} (corresponding to a high-to-medium emphasis on minimizing workload), while ALWAYS-QUERY performs the best for higher values of w_{task} (corresponding to a high emphasis on maximum task performance, which the ALWAYS-QUERY baseline achieves due to its lack of exploration compared to LINUCB-QG).

3) *Additional Details: generalization on D_2 :* In this experiment, the validation process is analogous to that for the previous simulation results, but on the test set, we use separate workload models for LINUCB-QG action-selection, and for computing the evaluation metrics ΔWL and M_{wt} . We use either $f_{1, sim}$ or $f_{1,2, sim}$ for the action-selection workload model, while we fix the evaluation workload model to be $f_{2, sim}$, and refer to the two settings as f_1 -on- f_2 and $f_{1,2}$ -on- f_2 , respectively. Table VII shows the results for LINUCB-QG in each of the two settings.

As mentioned in Section VI-A, we find that the mean weighted metric M_{wt} is higher in the $f_{1,2}$ -on- f_2 than the f_1 -on- f_2 setting (and ΔWL and f_q are both lower).

	ΔWL	t_{conv}	$f_{fail,food}$	$f_{auto,food}$
Workload Model $f_{1,sim}$				
-LINUCB	-0.50 ± 0.00	3.32 ± 1.04	0.00 ± 0.00	1.00 ± 0.00
-ALWAYSQUERY	-0.33 ± 0.09	1.68 ± 0.39	0.00 ± 0.00	0.00 ± 0.00
-LINUCB-EXPDECAY	-0.50 ± 0.00	2.70 ± 0.93	0.02 ± 0.05	0.54 ± 0.17
-LINUCB-QG	-0.47 ± 0.06	2.28 ± 0.60	0.00 ± 0.00	0.20 ± 0.22
Workload Model $f_{2,sim}$				
-LINUCB	-0.50 ± 0.00	3.32 ± 1.04	0.00 ± 0.00	1.00 ± 0.00
-ALWAYSQUERY	0.15 ± 0.43	1.68 ± 0.39	0.00 ± 0.00	0.00 ± 0.00
-LINUCB-EXPDECAY	-0.48 ± 0.08	3.54 ± 1.01	0.00 ± 0.00	0.84 ± 0.15
-LINUCB-QG	-0.50 ± 0.00	3.24 ± 1.03	0.00 ± 0.00	0.92 ± 0.10
Workload Model $f_{1,2,sim}$				
-LINUCB	-0.46 ± 0.00	3.32 ± 1.04	0.00 ± 0.00	1.00 ± 0.00
-ALWAYSQUERY	0.15 ± 0.43	1.68 ± 0.39	0.00 ± 0.00	0.00 ± 0.00
-LINUCB-EXPDECAY	-0.42 ± 0.19	3.54 ± 1.01	0.00 ± 0.00	0.84 ± 0.15
-LINUCB-QG	-0.45 ± 0.02	2.68 ± 0.70	0.00 ± 0.00	0.56 ± 0.27

TABLE III: Additional convergence metrics in simulation on the test set, corresponding to $w_{task} = 0.4$, for 3 different data regimes in the workload model, averaged across 5 seeds (For LINUCB-EXPDECAY, we also average across 5 policy random seeds). Metric values for LINUCB-EXPDECAY and LINUCB-QG correspond to the hyperparameter setting with maximal M_{wt} on the validation set (for each separate data setting).

w_{task}	Method	$r_{task,avg}$	M_{wt}	f_q
0.2	LINUCB	0.35 ± 0.15	0.47 ± 0.03	0.00 ± 0.00
	ALWAYSQUERY	0.64 ± 0.19	0.39 ± 0.05	1.00 ± 0.00
	LINUCB-EXPDECAY	0.39 ± 0.17	0.48 ± 0.03	0.44 ± 0.15
	LINUCB-QG	0.48 ± 0.18	0.47 ± 0.02	0.80 ± 0.22
0.3	LINUCB	0.35 ± 0.15	0.45 ± 0.04	0.00 ± 0.00
	ALWAYSQUERY	0.64 ± 0.19	0.42 ± 0.05	1.00 ± 0.00
	LINUCB-EXPDECAY	0.39 ± 0.17	0.47 ± 0.05	0.44 ± 0.15
	LINUCB-QG	0.48 ± 0.18	0.47 ± 0.01	0.80 ± 0.22
0.5	LINUCB	0.35 ± 0.15	0.42 ± 0.07	0.00 ± 0.00
	ALWAYSQUERY	0.64 ± 0.19	0.49 ± 0.07	1.00 ± 0.00
	LINUCB-EXPDECAY	0.39 ± 0.17	0.45 ± 0.08	0.44 ± 0.15
	LINUCB-QG	0.48 ± 0.18	0.48 ± 0.06	0.80 ± 0.22
0.6	LINUCB	0.35 ± 0.15	0.41 ± 0.09	0.00 ± 0.00
	ALWAYSQUERY	0.64 ± 0.19	0.52 ± 0.09	1.00 ± 0.00
	LINUCB-EXPDECAY	0.43 ± 0.18	0.45 ± 0.11	0.56 ± 0.15
	LINUCB-QG	0.48 ± 0.18	0.48 ± 0.08	0.80 ± 0.22
0.7	LINUCB	0.35 ± 0.15	0.39 ± 0.10	0.00 ± 0.00
	ALWAYSQUERY	0.64 ± 0.19	0.55 ± 0.11	1.00 ± 0.00
	LINUCB-EXPDECAY	0.43 ± 0.18	0.45 ± 0.13	0.56 ± 0.15
	LINUCB-QG	0.48 ± 0.18	0.48 ± 0.11	0.80 ± 0.22
0.8	LINUCB	0.35 ± 0.15	0.38 ± 0.12	0.00 ± 0.00
	ALWAYSQUERY	0.64 ± 0.19	0.58 ± 0.14	1.00 ± 0.00
	LINUCB-EXPDECAY	0.43 ± 0.18	0.44 ± 0.14	0.56 ± 0.15
	LINUCB-QG	0.48 ± 0.18	0.48 ± 0.13	0.80 ± 0.22
0.9	LINUCB	0.35 ± 0.15	0.36 ± 0.13	0.00 ± 0.00
	ALWAYSQUERY	0.64 ± 0.19	0.61 ± 0.16	1.00 ± 0.00
	LINUCB-EXPDECAY	0.43 ± 0.18	0.44 ± 0.16	0.56 ± 0.15
	LINUCB-QG	0.48 ± 0.18	0.48 ± 0.15	0.80 ± 0.22

TABLE IV: Workload data setting $f_{1,sim}$: Querying bandit algorithm metrics in simulation on the test set for different values of w_{task} . Averages are across 5 random seeds (For LINUCB-EXPDECAY, we also average across 5 policy random seeds). Metric values for LINUCB-EXPDECAY and LINUCB-QG correspond to the hyperparameter setting with maximal M_{wt} on the validation set (for each separate data setting).

It is also the case that M_{wt} is slightly higher in $f_{1,2}$ -on- f_2 compared to the f_2 -on- f_2 case (that is, the value shown in the $f_{2,sim}$ section of Table I, for LINUCB-QG). This is because training on $D_{1,2}$ leads to selecting a less conservative policy that queries more but keeps workload low (compared to training on D_2).

4) *Sample Workload Model Rollout*: Finally, Figure 5 shows a rollout of the workload model in simulation for LINUCB-QG, showing how the workload WL_t evolves over time, how the UCB estimate gap variable G varies, and when

LINUCB-QG decides to query. In this example, LINUCB-QG decides to ask the human for help when $G > wWL_t$ (in this rollout, $w = 4$), but also recall that once LINUCB-QG has asked for help for the current food item, it will continue to execute the expert action until it has converged.

I. Experiments: Real-world User Study

1) *Feeding Tool*: In our work, we use a custom feeding tool developed in prior work [9, 42], which is attached to the end of the Kinova’s Robotiq 2F-85 gripper. The tool consists

w_{task}	Method	$r_{task,avg}$	M_{wt}	f_q
0.2	LINUCB	0.35 ± 0.15	0.47 ± 0.03	0.00 ± 0.00
	ALWAYSQUERY	0.64 ± 0.19	0.01 ± 0.33	1.00 ± 0.00
	LINUCB-EXPDECAY	0.31 ± 0.12	0.45 ± 0.07	0.16 ± 0.15
	LINUCB-QG	0.35 ± 0.14	0.47 ± 0.03	0.08 ± 0.10
0.3	LINUCB	0.35 ± 0.15	0.45 ± 0.04	0.00 ± 0.00
	ALWAYSQUERY	0.64 ± 0.19	0.08 ± 0.27	1.00 ± 0.00
	LINUCB-EXPDECAY	0.31 ± 0.12	0.43 ± 0.06	0.16 ± 0.15
	LINUCB-QG	0.35 ± 0.14	0.46 ± 0.04	0.08 ± 0.10
0.5	LINUCB	0.35 ± 0.15	0.42 ± 0.07	0.00 ± 0.00
	ALWAYSQUERY	0.64 ± 0.19	0.24 ± 0.18	1.00 ± 0.00
	LINUCB-EXPDECAY	0.31 ± 0.12	0.40 ± 0.06	0.16 ± 0.15
	LINUCB-QG	0.35 ± 0.14	0.43 ± 0.07	0.08 ± 0.10
0.6	LINUCB	0.35 ± 0.15	0.41 ± 0.09	0.00 ± 0.00
	ALWAYSQUERY	0.64 ± 0.19	0.32 ± 0.14	1.00 ± 0.00
	LINUCB-EXPDECAY	0.31 ± 0.12	0.38 ± 0.07	0.16 ± 0.15
	LINUCB-QG	0.35 ± 0.14	0.41 ± 0.09	0.08 ± 0.10
0.7	LINUCB	0.35 ± 0.15	0.39 ± 0.10	0.00 ± 0.00
	ALWAYSQUERY	0.64 ± 0.19	0.40 ± 0.12	1.00 ± 0.00
	LINUCB-EXPDECAY	0.43 ± 0.18	0.41 ± 0.10	0.56 ± 0.15
	LINUCB-QG	0.40 ± 0.07	0.35 ± 0.08	0.76 ± 0.20
0.8	LINUCB	0.35 ± 0.15	0.38 ± 0.12	0.00 ± 0.00
	ALWAYSQUERY	0.64 ± 0.19	0.48 ± 0.12	1.00 ± 0.00
	LINUCB-EXPDECAY	0.43 ± 0.18	0.42 ± 0.13	0.56 ± 0.15
	LINUCB-QG	0.40 ± 0.07	0.37 ± 0.07	0.76 ± 0.20
0.9	LINUCB	0.35 ± 0.15	0.36 ± 0.13	0.00 ± 0.00
	ALWAYSQUERY	0.64 ± 0.19	0.56 ± 0.15	1.00 ± 0.00
	LINUCB-EXPDECAY	0.43 ± 0.18	0.42 ± 0.15	0.56 ± 0.15
	LINUCB-QG	0.40 ± 0.07	0.38 ± 0.07	0.76 ± 0.20

TABLE V: Workload data setting $f_{2,sim}$: Querying bandit algorithm metrics in simulation on the test set for different values of w_{task} . Averages are across 5 random seeds (For LINUCB-EXPDECAY, we also average across 5 policy random seeds). Metric values for LINUCB-EXPDECAY and LINUCB-QG correspond to the hyperparameter setting with maximal M_{wt} on the validation set (for each separate data setting).

w_{task}	Method	$r_{task,avg}$	M_{wt}	f_q
0.2	LINUCB	0.35 ± 0.15	0.44 ± 0.03	0.00 ± 0.00
	ALWAYSQUERY	0.64 ± 0.19	0.01 ± 0.32	1.00 ± 0.00
	LINUCB-EXPDECAY	0.31 ± 0.12	0.40 ± 0.15	0.16 ± 0.15
	LINUCB-QG	0.40 ± 0.12	0.44 ± 0.03	0.44 ± 0.27
0.3	LINUCB	0.35 ± 0.15	0.43 ± 0.04	0.00 ± 0.00
	ALWAYSQUERY	0.64 ± 0.19	0.08 ± 0.27	1.00 ± 0.00
	LINUCB-EXPDECAY	0.31 ± 0.12	0.39 ± 0.13	0.16 ± 0.15
	LINUCB-QG	0.40 ± 0.12	0.44 ± 0.04	0.44 ± 0.27
0.5	LINUCB	0.35 ± 0.15	0.40 ± 0.07	0.00 ± 0.00
	ALWAYSQUERY	0.64 ± 0.19	0.24 ± 0.18	1.00 ± 0.00
	LINUCB-EXPDECAY	0.31 ± 0.12	0.37 ± 0.10	0.16 ± 0.15
	LINUCB-QG	0.40 ± 0.12	0.43 ± 0.06	0.44 ± 0.27
0.6	LINUCB	0.35 ± 0.15	0.39 ± 0.09	0.00 ± 0.00
	ALWAYSQUERY	0.64 ± 0.19	0.32 ± 0.14	1.00 ± 0.00
	LINUCB-EXPDECAY	0.31 ± 0.12	0.36 ± 0.09	0.16 ± 0.15
	LINUCB-QG	0.40 ± 0.12	0.42 ± 0.07	0.44 ± 0.27
0.7	LINUCB	0.35 ± 0.15	0.38 ± 0.10	0.00 ± 0.00
	ALWAYSQUERY	0.64 ± 0.19	0.40 ± 0.12	1.00 ± 0.00
	LINUCB-EXPDECAY	0.31 ± 0.12	0.35 ± 0.09	0.16 ± 0.15
	LINUCB-QG	0.40 ± 0.12	0.42 ± 0.08	0.44 ± 0.27
0.8	LINUCB	0.35 ± 0.15	0.37 ± 0.12	0.00 ± 0.00
	ALWAYSQUERY	0.64 ± 0.19	0.48 ± 0.12	1.00 ± 0.00
	LINUCB-EXPDECAY	0.43 ± 0.18	0.38 ± 0.12	0.56 ± 0.15
	LINUCB-QG	0.41 ± 0.05	0.34 ± 0.08	0.76 ± 0.20
0.9	LINUCB	0.35 ± 0.15	0.36 ± 0.13	0.00 ± 0.00
	ALWAYSQUERY	0.64 ± 0.19	0.56 ± 0.15	1.00 ± 0.00
	LINUCB-EXPDECAY	0.43 ± 0.18	0.40 ± 0.15	0.56 ± 0.15
	LINUCB-QG	0.41 ± 0.05	0.37 ± 0.04	0.76 ± 0.20

TABLE VI: Workload data setting $f_{1,2,sim}$: Querying bandit algorithm metrics in simulation on the test set for different values of w_{task} . Averages are across 5 random seeds (For LINUCB-EXPDECAY, we also average across 5 policy random seeds). Metric values for LINUCB-EXPDECAY and LINUCB-QG correspond to the hyperparameter setting with maximal M_{wt} on the validation set (for each separate data setting).

Metric	f_1 -on- f_2	$f_{1,2}$ -on- f_2
$r_{task,avg}$	0.48 ± 0.18	0.40 ± 0.12
ΔWL	-0.13 ± 0.37	-0.50 ± 0.00
M_{wt}	0.27 ± 0.16	0.46 ± 0.05
f_q	0.80 ± 0.22	0.44 ± 0.27

TABLE VII: LINUCB-QG performance in cross-data setting at test time, showing algorithm metrics in simulation on the test set, with $w_{task} = 0.4$. Averages are across 5 random seeds. Values for $r_{task,avg}$ and ΔWL correspond to the hyperparameter setting with maximal M_{wt} on the validation set (for each separate data setting).

of a motorized fork with two degrees of freedom: pitch β and roll γ . Each of the six robot actions a_r (for $r \in \{1, \dots, 6\}$) corresponds to a unique value of β and γ . In particular, the pitch configuration (either TA, VS, or TV) affects the value of β , while the roll configuration (either 0° or 90°) affects the value of γ .

2) *Details on Perception Modules:* To more accurately determine skewering-relevant geometric information for each bite-sized food item, we leverage perception modules that were developed in prior work [42]. We use GroundingDINO [43] to produce an initial bounding box around the food item, followed by SAM [44] to segment the food item, and finally extract the minimum area rectangle around the segmentation mask to get a refined bounding box. From this bounding box, we derive the centroid and major axis of the food item, which are used by the low-level action executor to execute the desired robot action a_r .

3) *Additional Details and Analysis:* Here we present additional details related to the real-world user study experiments outlined in Section VI-B.

Pre-method questions. We ask the users with mobility limitations the following questions prior to each method:

- “How mentally/physically burdened do you feel currently?”
- “How hurried or rushed do you feel currently?”

For users without mobility limitations, we ask the following questions:

- “How mentally burdened do you feel currently?”
- “How hurried or rushed do you feel currently?”

Post-method questions. We ask the users with mobility limitations the following questions after each method:

- “For the last method, how mentally/physically burdened do you feel currently because of the robot querying you?”
- “For the last method, how hurried or rushed do you feel currently because of the robot querying you?”
- “For the last method, how hard did you have to work to make the robot pick up food items?”
- “For the last method, how successful was the robot in picking up food items?”

For users without mobility limitations, we ask the following questions:

- “For the last method, how mentally burdened do you feel currently because of the robot querying you?”
- “For the last method, how hurried or rushed do you feel currently because of the robot querying you?”
- “For the last method, how hard did you have to work to make the robot feed you?”

- “For the last method, how successful was the robot in picking up the food item and bringing it to your mouth?”

Compensation. Users were compensated at a rate of \$12/hr, for a total compensation of \$18 for the entire study (as the study duration was 1.5 hr).

Note on initial workload WL_0 . Although we do ask for an initial estimate of the user’s workload by asking the pre-method questions above, in our real-world experiments, we provide a fixed initial workload value of $WL_0 = 0.5$ for LINUCB-QG. This value is used by LINUCB-QG for its internal workload predictions and decision-making. However, when calculating the subjective metrics in Section VI-B that measure changes in workload (Delta-Mental, Delta-Temporal, and Delta-Querying Workload), we use the responses to the pre-method questions to estimate the user’s initial workload.

Method comparison across all metrics. Tables VIII and IX include comparisons across the three methods used in the real-world user study (LINUCB, ALWAYSQUERY, LINUCB-QG) for the 7 subjective and 3 objective metrics mentioned in Section VI-B, respectively. For all metrics, we find that LINUCB-QG achieves an intermediate value for that metric compared to the other two algorithms, suggesting that our method finds a balance between querying workload and task performance (which these metrics cover). Additionally, Table X shows the full results of the Wilcoxon paired signed-rank tests that we used to determine whether LINUCB-QG exhibited statistically significant differences in the full set of metrics compared to LINUCB-QG and ALWAYSQUERY. For the metrics related to querying workload, our alternative hypothesis was that the value of the metric for LINUCB-QG was less than the value for ALWAYSQUERY. For the metrics related to task performance, our alternative hypothesis was that the value of the metric for LINUCB-QG was greater than the value for LINUCB. For all metrics, we find that LINUCB-QG has a statistically significant improvement compared to the baseline for that metric.

Comments on Post-Performance metric. When looking at the Post-Performance metric, we find that LINUCB-QG achieves an intermediate value, higher than LINUCB but lower than ALWAYS-QUERY. When asking users to rate subjective success, we asked them to rate the overall success of each algorithm, which depends on both whether the algorithm successfully picked up food items and how many attempts were required for success. For this reason, we believe that users rated the success of ALWAYS-QUERY highly because it efficiently selects the optimal action for each food item within one timestep, whereas LINUCB-QG sometimes takes multiple timesteps if it does not query for a particular food item.

ACKNOWLEDGMENT

This work was partly funded by NSF CCF 2312774 and NSF OAC-2311521, a LinkedIn Research Award, and a gift from Wayfair, and by NSF IIS 2132846 and CAREER 2238792. Research reported in this publication was additionally supported by the Eunice Kennedy Shriver National

Method	Post-Mental	Post-Temporal	Post-Performance	Post-Effort	Delta-Mental	Delta-Temporal	Delta-Querying Workload
LINUCB	1.24 ± 0.59	1.37 ± 0.97	3.03 ± 0.77	1.24 ± 0.75	-0.34 ± 0.88	-0.26 ± 0.92	-0.02 ± 0.16
ALWAYSQUERY	3.03 ± 1.38	2.58 ± 1.55	4.67 ± 0.72	3.03 ± 1.33	1.42 ± 1.39	0.87 ± 1.76	0.39 ± 0.31
LINUCB-QG	2.26 ± 1.11	2.08 ± 1.22	4.06 ± 1.04	2.24 ± 1.05	0.63 ± 1.05	0.37 ± 1.08	0.21 ± 0.20

TABLE VIII: Subjective metric results for the real-world user study.

Method	$r_{task,avg}$	$n_{success}$	n_q
LINUCB	0.38 ± 0.08	2.00 ± 0.23	-
ALWAYSQUERY	0.87 ± 0.25	2.68 ± 0.61	3 ± 0
LINUCB-QG	0.68 ± 0.29	2.53 ± 0.72	1.74 ± 0.78

TABLE IX: Objective metric results for the real-world user study.

Metric	Hypothesis	p
Post-Mental	LINUCB-QG < ALWAYSQUERY	3.28e-4
Post-Temporal		1.42e-2
Post-Effort		1.2e-4
Delta-Mental		7.68e-4
Delta-Temporal		1.82e-2
Delta-Querying Workload		1.47e-4
n_q		2.93e-7
Post-Performance	LINUCB-QG > LINUCB	1.59e-4
$r_{task,avg}$		1.56e-4
$n_{success}$		2.18e-4

TABLE X: Wilcoxon paired signed-rank test results for the real-world user study, showing p -values associated with querying workload metrics (top) and task performance metrics (bottom). For all tests, we used a significance level of $\alpha = 0.05$.

Institute Of Child Health & Human Development of the National Institutes of Health and the Office of the Director of the National Institutes of Health under Award Number T32HD113301. The content is solely the responsibility of the authors and does not necessarily represent the official views of the National Institutes of Health.

The authors would like to thank Ethan Gordon for his assistance with the food dataset, Ziang Liu, Pranav Thakkar and Rishabh Madan for their help with running the robot user study, Janna Lin for providing the voice interface, Shuaixing Chen for helping with figure creation, Tom Silver for paper feedback, and all of the participants in our two user studies.